Biophysical Chemistry 185 (2014) 47–57

Contents lists available at ScienceDirect

Biophysical Chemistry

journal homepage: http://www.elsevier.com/locate/biophyschem

# Length-dependent conformational transitions of polyglutamine repeats as molecular origin of fibril initiation

Benjamin S. Heck, Franziska Doll, Karin Hauser *

*Department of Chemistry and Konstanz Research School Chemical Biology, University of Konstanz, 78457 Konstanz, Germany*

## HIGHLIGHTS

- Molecular mechanisms of polyglutamine diseases have been studied spectroscopically.
- The glutamine repeat length is directly correlated to β-sheet formation.
- The concentration is another critical factor influencing the polyQ conformation.
- Different β-structures indicate different steps in polyQ fibrillogenesis.

## GRAPHICAL ABSTRACT

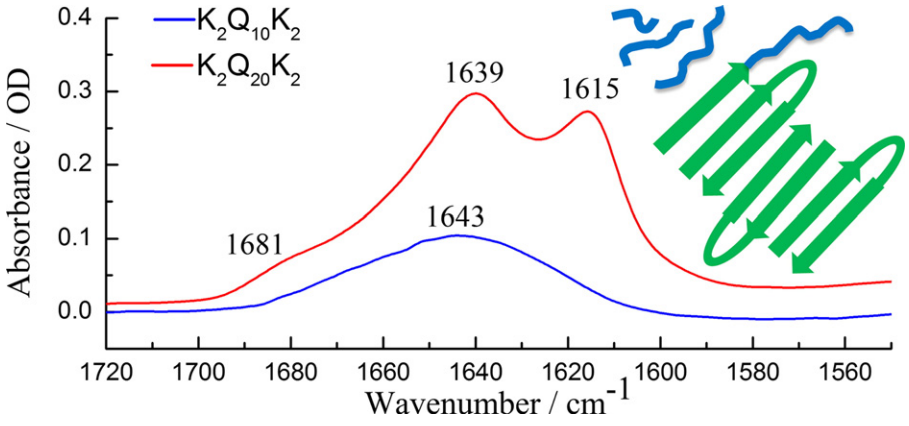


## ARTICLE INFO

*Article history:*
Received 30 September 2013
Received in revised form 15 November 2013
Accepted 18 November 2013
Available online 26 November 2013

*Keywords:*
Polyglutamine
Conformation
Fibril formation
Peptides
IR
CD

## ABSTRACT

Polyglutamine (polyQ) sequences are found in a variety of proteins with normal function. However, their repeat expansion is associated with a number of neurodegenerative diseases, also called polyQ diseases. The length of the polyQ sequence, varying in the number of consecutive glutamines among different diseases, is critical for inducing fibril formation. We performed a systematic spectroscopic study to analyze the conformation of polyQ model peptides in dependence of the glutamine sequence lengths ($K_2Q_nK_2$ with $n = 10, 20, 30$). Complementary FTIR- and CD-spectra were measured in a wide concentration range and repeated heating and cooling cycles revealed the thermal stability of formed β-sheets. The shortest glutamine sequence $K_2Q_{10}K_2$ shows solely random structure for concentrations up to 10 mg/ml. By increasing the peptide length to $K_2Q_{20}K_2$, a significant fraction of β-sheet is observed even at low concentrations of 0.01 mg/ml. The higher the concentration, the more the structural composition is dominated by the intermolecular β-sheet. The formation of highly thermostable β-sheet is much more pronounced in $K_2Q_{30}K_2$. $K_2Q_{30}K_2$ precipitates at a concentration of 0.3 mg/ml. Our spectroscopic study shows that the aggregation tendency is enhanced with increased glutamine repeat expansion and that the concentration plays another critical factor in the β-sheet formation.



## 1. Introduction

The implication of polyglutamine (polyQ) repeats in proteins have become obvious by disease patterns. There are at least ten inherited polyQ diseases including the well-known Huntington's disease [1]. The proteins associated with polyQ diseases show no sequence

* Corresponding author. Tel.: +49 7531 885356; fax: +49 7531 883139.
*E-mail address:* Karin.Hauser@uni-konstanz.de (K. Hauser).

0301-4622/$ – see front matter © 2013 Elsevier B.V. All rights reserved.
http://dx.doi.org/10.1016/j.bpc.2013.11.008

homology except for an expanded polyQ region. There is a pathogenic threshold of repeat length that varies somewhat among diseases, but is generally in the range of 35–40 consecutive glutamines and the length of the polyQ sequence determines the age of the disease onset [2,3]. The processes of protein misfolding and aggregation seem to be a direct cause of neurodegeneration [4]. However, the molecular mechanisms that drive folding, misfolding or aggregation of a polyQ sequence are little understood. It is agreed that the length of the polyglutamine chain is a crucial factor for aggregation and disease. Structural properties of polyQ repeats in dependence of their sequence length are thus important for understanding the molecular mechanisms that are associated with a normal or abnormal biological function of polyQ proteins. Synthesized polyQ peptides have been used to analyze folding, misfolding and aggregation of polyQ repeats. However, detailed structure information has been difficult to obtain because polyQ peptides are quite insoluble. The observation that polyQ peptides tend to aggregate was already shown in an early study on synthetic polymers which are insoluble in water and readily aggregate to form viscous gels through the formation of interamide hydrogen bonds [5]. The first structure model of polyQ was proposed by Perutz et al. [6] who suggested that polyQ sequences could form polar zippers made of antiparallel β-strands held together by hydrogen bonds between main-chain and side-chain amides. These studies used synthetic polyQ peptides with 15 glutamines made soluble by the inclusion of flanking charged residues (Asp2-Gln15-Lys2). In subsequent experiments it was postulated that shorter polyQ tracts have a random coil conformation whereas longer repeats form β-sheet structures. A β-helix was suggested comprising about 20 Q residues per helical turn [7]. Other studies of polyQ peptides with repeat lengths from 5 to 44 Q residues indicated that, irrespective of their length, all peptides are in random structure [8]. This observation suggested that the existence of a disease threshold is not related to a conformational change in the monomeric state, but rather the threshold could be explained by the propensity of longer polyQ sequences to aggregate. A possible explanation for contradictions about structural states of polyQ peptides could be that random coil conformation is only observed when the solvent induces full solubility of the polyQ stretches, while β-sheet structures are observed when polyQ is partially aggregated. A method was described for dissolving and disaggregating chemically synthesized polyQ peptides up to a length of 44 glutamines by a mixture of trifluoroacetic acid (TFA) and hexafluoroisopropanol (FFIP) [9]. Other structure investigations of polyQ aggregates were carried out by use of polyQ peptides in which at different sequence intervals Gln–Gln pairs were replaced by Pro-Gly pairs, elements that are expected to favor β-turns and are incompatible with extended β-sheet chains [10]. The results indicate that polyQ aggregates consist of alternating elements of extended chains and turns, thus suggesting an antiparallel β-sheet folding motif as the fundamental aggregation repeat unit.

A model of polyQ aggregate initiation and elongation was proposed where an unstructured polyQ monomer serves as nucleus and undergoes a structural transition to a four-stranded antiparallel β-sheet before elongation [11]. Other mechanisms have been proposed how glutamines are involved in aggregation, one involving intrasheet hydrogen bonding of their side-chain amide groups (polar zipper model) [6], and a second involving reorientation of intrasheet glutamine hydrogen bonding resulting in close van der Waals contacts between the glutamine methylene groups (steric zipper model) [12]. Model β-hairpin systems have been designed to analyze which interactions are involved in early assembly processes [13].

Fret studies analyzed the role of polyQ length on the aggregation [14]. It was shown that the peptides become increasingly collapsed as the number of glutamines increased with an estimated effective persistence length decreasing from ~11 Å to ~7 Å as the numbers of glutamines increased from 8 to 24. Molecular dynamics simulations made also predictions about the length dependence of the polyQ-mediated aggregation states. It was concluded that the longer the glutamine tract length, the higher is the propensity to form β-helices [15–18]. A mechanism for protein aggregation has been proposed by simulations where expanded polyQ tracts destabilize the affected proteins by the formation of partially intermediate states [19].

From the above summarized studies, it becomes obvious that different models about aggregation mechanisms of polyQ proteins exist. A reason therefore is given by the fact that the conformational transitions are influenced by the used residue sequence and/or the specific measurement conditions. Since a common property of all polyQ diseases is an abnormal extended glutamine sequence in the polyQ protein, polyQ peptides consisting primarily out of glutamine residues are ideal model systems to study their conformational properties [20]. Here we report a systematic spectroscopic study to get insight into the molecular origin for fibril initiation. The studied peptides differ only in the glutamine sequence length varying between 10, 20 and 30 consecutive glutamines. The impact of the concentration on the conformation, the thermal stability of formed β-sheets and the conformational influence of the flanking charged lysine residues are analyzed in detail by complementary FTIR- and CD-measurements. Both approaches facilitate marker-free conformational studies of polyQ repeats under physiological conditions and contribute to understand the molecular mechanism of fibrillogenesis in polyQ proteins.

## 2. Experimental section

### 2.1. Peptides

PolyQ peptides were synthesized by Peptide Specialty Laboratories GmbH (Heidelberg, Germany) using FMOC-based solid-state synthesis methods. The studied peptides vary in the glutamine sequence lengths and are denominated as $K_2Q_nK_2$ with n = 10, 20, 30. Two lysines were introduced at each terminus to enhance the solubility. The peptides were lyophilized and dissolved in $D_2O$, resulting in an acidic pD of ~2.9. $K_2Q_{30}K_2$ doesn't dissolve even at concentrations of 0.1 mg/ml and was treated with ultrasound for 30 min directly before the measurement. For the pD study, the pD was adjusted by adding DCl, $D_3PO_4$ or NaOD and measured with a pH electrode using the conversion pD = pH + 0.4 [21].

### 2.2. CD sample preparations and CD measurements

$K_2Q_nK_2$ peptides were dissolved at the desired concentration in either $H_2O$ or $D_2O$. CD measurements were carried out with a J815 spectrometer (JASCO, USA). Data were recorded between 300 nm and 180 nm with a scanning speed of 200 nm/min and a digital integration time of 0.25 s. The bandwidth was 1 nm. Final spectra were recorded as an average of seven scans, smoothed and a smoothed water background spectrum was subtracted. Variable-temperature experiments were performed with a 1 °C/min ramp speed and the temperature was controlled by a regulated flow from a water bath (FL300, Julabo, Germany) through a cell holder. 1 mm quartz cells (Starna) were used except for peptide concentrations of 0.01 mg/ml and 0.03 mg/ml that were analyzed with 1 cm cell path length. A heating run was carried out from 5 °C to 90 °C in steps of 5 °C.

### 2.3. IR sample preparation and FTIR measurements

For IR measurements, the peptides were dissolved in 0.1 M DCl and lyophilized three times to remove the trifluoroacetic acid (TFA) counterions remaining from the peptide synthesis. TFA absorbs at 1672 $cm^{-1}$ [22] and thus interferes the analyzed amide I′ region. The samples were redissolved in $D_2O$ after the lyophilization procedure. $D_2O$ is used as solvent for all IR measurements since $H_2O$ has a strong absorption of the HO bending vibration at ~1650 $cm^{-1}$ overlaying the amide I region (1600–1700 $cm^{-1}$). Due to the mass effect on the vibrational frequency, the DO bending vibration is shifted to ~1200 $cm^{-1}$ and thus out of the amide I region. The amide I band, mainly the C═O stretching vibration

of the polypeptide backbone, is used for secondary structure analysis and is termed as amide I′ if the peptide/protein is dissolved in $D_2O$. FTIR experiments were performed with an Equinox 55 FTIR spectrometer (Bruker, Germany). Peptide solutions were sealed in a homemade demountable cell with $CaF_2$ windows separated by a spacer with 10 μm or 100 μm path length. Spectra were acquired from 6000 $cm^{-1}$ to 1000 $cm^{-1}$ with a resolution of 4 $cm^{-1}$. 128 scans were recorded and averaged for each spectrum. The sample temperature was controlled with a water bath (Ecoline-E300, Lauda, Germany) connected to the cell holder. Using a home-built shuttle device, the sample and reference positions were moved alternately to measure the sample and reference spectra for each temperature successively. Determining the spectra and reference spectra simultaneously and purging the instrument with dry air avoids the requirement of water vapor correction. The polyQ peptides were measured at different temperatures by an automated temperature control and acquisition macro, starting from 5 °C to 90 °C in steps of 5 °C. The $D_2O$ water background was subtracted for each temperature using a self-written MATLAB script.

## 3. Results and discussion

The conformation and conformational stability of the polyQ peptides were studied in dependence of the glutamine sequence length by FTIR- and CD-spectroscopy. All peptides have the same design: a glutamine sequence varies between 10 and 30 consecutive residues and two lysine residues have been introduced at each terminus to enhance the solubility in aqueous solution. For secondary structure analysis, we analyzed the amide I′ band in the IR which consists mainly of the carbonyl stretching vibration of the peptide backbone absorbing between 1600 and 1700 $cm^{-1}$. Different secondary structure elements have characteristic amide I′ frequency regions (in $D_2O$): α-helices absorb between 1642 and 1660 $cm^{-1}$, random coil between 1639 and 1654 $cm^{-1}$ and β-sheets have a strong absorption band between 1615 and 1638 $cm^{-1}$ and a weaker band between 1672 and 1694 $cm^{-1}$ [23]. IR-spectroscopy, in contrast to CD spectroscopy, is very sensitive to monitor differences in β-sheet structures. Intra- and intermolecular β-sheets have been distinguished due to frequency shifts caused by different hydrogen bonding. β-strands in ordered or amorphous aggregates are often characterized by a significant increase in the splitting between the low and high frequency amide I′ components [24]. The side chain of the glutamine comprises another carbonyl group. Due to the coupling with the side chain $NH_2$ bending vibration it shows a strong sensitivity towards deuteration. Frequency downshifts from 1668 to 1687 $cm^{-1}$ in $H_2O$ towards 1635–1654 $cm^{-1}$ in $D_2O$ have been observed for of the glutamine side chain C═O stretching vibration [25]. However, the glutamine side chain and backbone C═O stretching vibrations both absorb in the same frequency region leading to a broad band with overlapping components. The side chain $NH_2$ bending vibration has been assigned in polyglutamine containing huntingtin fragments to a band near 1605 $cm^{-1}$ [26] and is expected to be shifted out of the amide I′ frequency region of 1600–1700 $cm^{-1}$ after H–D exchange. Further side chain vibrations of glutamine are not overlaying the amide I′ frequencies [25]. CD-spectroscopy is used as complementary secondary structure analysis method. In contrast to IR-spectroscopy, random coil and α-helical structures can clearly be distinguished with CD. The characteristic signature for α-helical structure is a negative band with two minima near 210 nm and 220 nm and a maximum near 190 nm. A random coil spectrum reveals one minimum near 200 nm and a weak maximum near 215 nm. A characteristic β-sheet spectrum has a maximum in the region 195–200 nm and a minimum in the region 215–220 nm. However, changes in β-structures involved in fibril formation cannot be detected as sensitive as in the IR that reveals different hydrogen bonding of intra- and intermolecular β-sheets by observable amide I frequency shifts. Concentrations can be reduced to μM in CD spectroscopy whereas mM concentrations are required for IR-measurements. Since aggregation processes depend on concentration, the peptide conformation has been studied at different concentrations. IR and CD measurements have been performed complementary, allowing to study a wide concentration range (10 mg/ml–0.001 mg/ml). If β-structures have been formed, the thermal stability has been analyzed. The influence of the flanking lysines on the conformation has been studied by varying the pD value.

### 3.1. Conformation in dependence of temperature and concentration

#### 3.1.1. $K_2Q_{10}K_2$

Temperature-dependent FTIR and CD spectra of $K_2Q_{10}K_2$ at different concentrations are shown in Fig. 1. The FTIR absorption band with a maximum at 1641 $cm^{-1}$ consists of the carbonyl stretching vibrations of the backbone (amide I′) and the glutamine side chains. The contribution of the side chain vibration to the band is significant due to a comparable number of side chain and backbone carbonyls. Measurements in $H_2O$ reveal a band at ~1660 $cm^{-1}$ (data not shown). The significant frequency downshift to ~1641 $cm^{-1}$ in $D_2O$ reflects what has been observed for the glutamine side chain C═O stretching vibration before [25,26]. However, the backbone amide I′ components providing secondary structure information also contribute to the band at 1641 $cm^{-1}$. Complementary CD-measurements reveal a random coil structure due to the characteristic band signature with a minimum at 198 nm and a weak maximum at 219 nm. Upon heating to 90 °C, the bands are slightly shifted, but no structural change occurs. After re-cooling, the band signatures are the same as before. It should be noted that the IR measurements at 1 mg/ml concentration have been performed with an optical pathlength of 100 μm whereas 10 μm was used for 10 mg/ml concentration thus leading to the same absorption value. Decreasing the concentration to 0.1 mg/ml (55 μM) doesn't lead to a significant change. The CD spectra with a negative band at 197 nm and a weak positive band at 219 nm still indicate solely random coil structure. Summarizing, the short polyQ sequence $K_2Q_{10}K_2$ reveals a random structure in a wide concentration range (0.1–10 mg/ml) and doesn't form β-structures.

#### 3.1.2. $K_2Q_{20}K_2$

It becomes obvious that a structural change occurs when the sequence is elongated from 10 to 20 glutamines. Fig. 2 shows FTIR spectra of $K_2Q_{10}K_2$ and $K_2Q_{20}K_2$ measured at the same concentration of 10 mg/ml concentration at room temperature. The band at 1641 $cm^{-1}$ of $K_2Q_{10}K_2$ was assigned to the carbonyl side chain and random structure (Fig. 1). $K_2Q_{20}K_2$ reveals a slightly shifted band at 1639 $cm^{-1}$ and additional bands at 1615 $cm^{-1}$ and 1681 $cm^{-1}$ indicative for β-sheet with the characteristic two components of the amide I' band (Fig. 2). 1615 $cm^{-1}$ is at relatively low frequency what hints intermolecular β-sheet between the $K_2Q_{20}K_2$ monomers.

FTIR- and CD spectra of $K_2Q_{20}K_2$ have been performed at different concentrations, FTIR at 10 mg/ml, 1 mg/ml and 0.3 mg/ml, and CD at 0.3 mg/ml, 0.15 mg/ml and 0.01 mg/ml (Figs. 3, 4, 5). Temperature-dependent spectra were recorded from 5 °C to 90 °C to get insights into the thermal stability of the formed β-sheets. At least two heating cycles have been performed. All FTIR spectra reveal bands at ~1640 $cm^{-1}$ and the β-sheet bands at ~1615 $cm^{-1}$ and 1681 $cm^{-1}$. The bands shift only slightly in frequency upon heating.

In the spectra at lower concentrations, a band component at ~1635 $cm^{-1}$ becomes obvious in the IR spectra (Figs. 4 and 6). It is indicative for another β-structure that is existent in the longer sequence $K_2Q_{20}K_2$. 1635 $cm^{-1}$ is tentatively assigned to intramolecular β-sheet and 1615 $cm^{-1}$ to intermolecular β-sheet. The heating cycles reveal another characteristic property: the band at 1615 $cm^{-1}$ decreases after the first heating cycle, in particularly observable at low concentrations, in contrast to further heating cycles that show reversible intensity changes. It seems that the extended intermolecular β-sheet is reduced to a certain degree by heating up once, whereas further heating/cooling cycles change the intensities in a reversible manner.

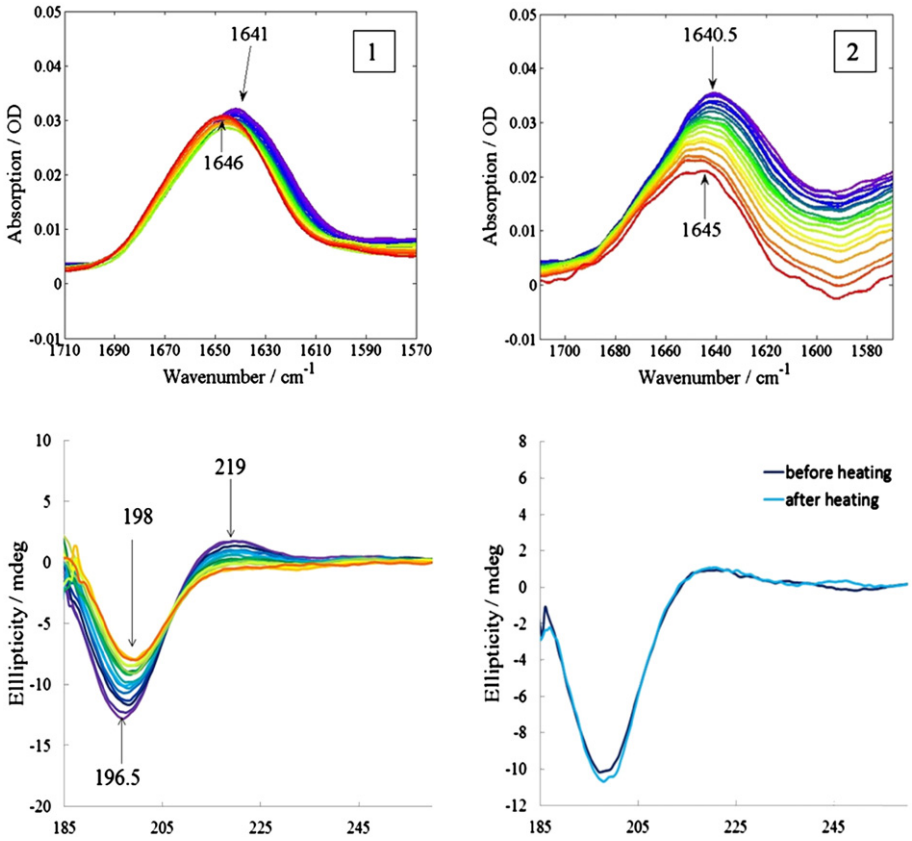


**Fig. 1.** Conformation of $K_2Q_{10}K_2$ measured from 5 °C (blue) to 90 °C (red) at various concentrations. Only random structure is observed. Upper panel: FTIR spectra at c = 10 mg/ml (left) and at c = 1 mg/ml (right). Lower panel: CD spectra with a concentration of 0.1 mg/ml at various temperatures (left) and at 20 °C before and after heating (right).

0.3 mg/ml was the lowest concentration feasible for both, FTIR- and CD-measurements (Fig. 4). The CD spectra at the same concentration show solely β-sheet with a band maximum at 196.5 nm and a minimum at 219 nm. After heating up to 90 °C and re-cooling again to 5 °C, the intensities at 195 nm and 219 nm are reduced, indicating a reduced amount of β-structure. The second heating cycle changes the structural composition only slightly as can be seen by the shoulder near 206 nm that indicates a small fraction of random structure.

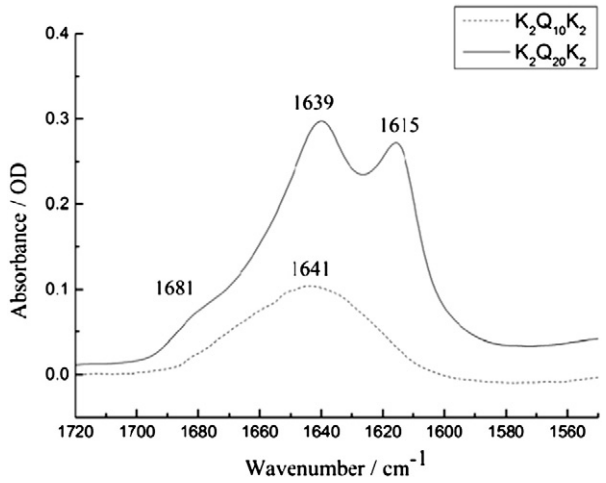


**Fig. 2.** FTIR spectra of $K_2Q_{10}K_2$ and $K_2Q_{20}K_2$, both measured at c = 10 mg/ml and at room temperature. A conformational change is observed for $K_2Q_{20}K_2$ revealing a structural composition of a significant fraction of β-sheet besides random structure.

When the concentration is reduced below 0.3 mg/ml, the fraction in random structure is significantly enhanced (Fig. 5). We observe again that heating $K_2Q_{20}K_2$ up once reduces the β-sheet fraction significantly for all concentrations below 1 mg/ml. After one heating cycle, the CD spectra at 0.15 mg/ml, 0.03 mg/ml and 0.01 mg/ml show conformations that don't change upon further heating cycles and that is dominated by random structure as seen by the minimum near 200 nm. However, β-sheet is still present indicated by the maximum near 195 nm and the minimum near 220 nm.

### 3.1.3. $K_2Q_{30}K_2$

The aggregation tendency is strongly increased in the extended glutamine sequence $K_2Q_{30}K_2$. At concentrations of 0.1 mg/ml, $K_2Q_{30}K_2$ precipitates. Therefore $K_2Q_{30}K_2$ samples were treated with ultrasound for 30 min directly before the measurement. FTIR- and CD-spectra were measured at 0.3 mg/ml (Figs. 6 and 7). Various bands are resolved in the FTIR spectra. As in $K_2Q_{10}K_2$ and $K_2Q_{20}K_2$, we assign the band at 1641 $cm^{-1}$ to the C═O stretching vibration of the glutamine side chain and fraction of random structure. The amide I′ bands at 1635 $cm^{-1}$ and 1614.5 $cm^{-1}$ are characteristic for β-structures. Upon heating from 5 °C to 90 °C, the frequency positions change only slightly, less than 3 $cm^{-1}$. As in $K_2Q_{20}K_2$, the amide I′ band at 1615 $cm^{-1}$ decreases after the first heating cycle but repeated heating cycles are reversible and do not impact the temperature-dependent intensities any more. Remarkably is the ratio between the amide I′ bands of 1643 $cm^{-1}$ and 1615 $cm^{-1}$ after the second heating cycle (Fig. 6). In contrast to $K_2Q_{20}K_2$, the band at 1615 $cm^{-1}$ is equal in intensity with the band at 1643 $cm^{-1}$. Thus the fraction of intermolecular β-sheets is significantly increased in $K_2Q_{30}K_2$ as compared to $K_2Q_{20}K_2$.

The CD spectra at the same concentration of 0.3 mg/ml (Fig. 7, upper panel) show a dominating and highly thermostable β-structure with a

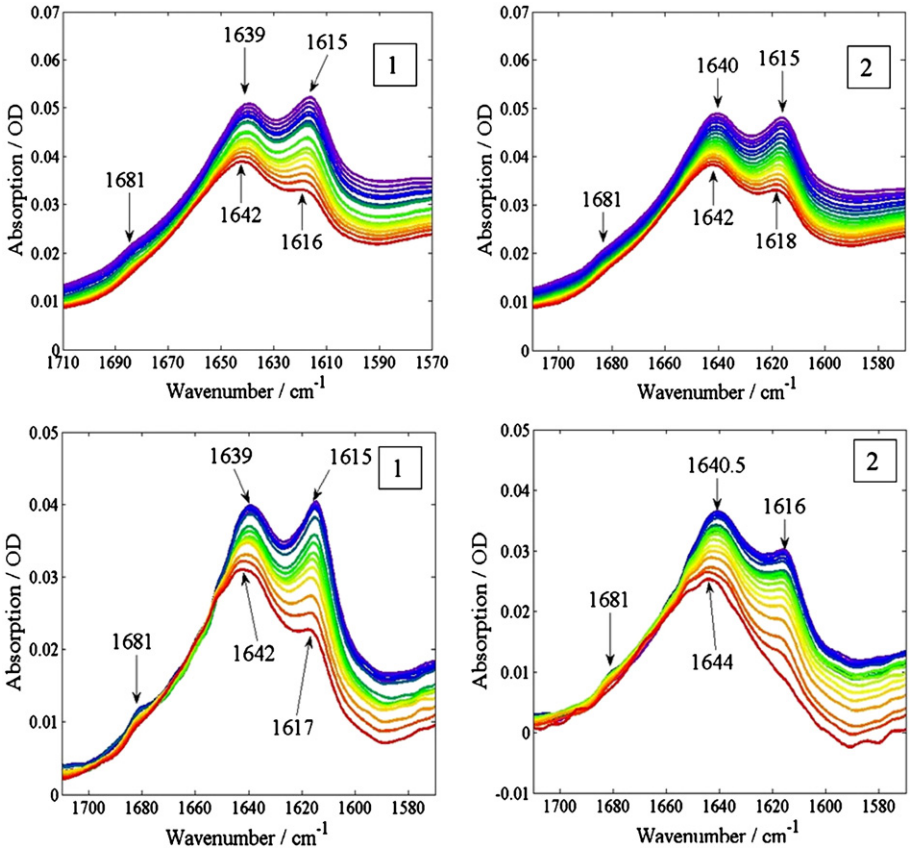


**Fig. 3.** FTIR spectra of $K_2Q_{20}K_2$ measured from 5 °C (blue) to 90 °C (red). Upper panel: c = 10 mg/ml; first (left) and second (right) heating cycle. Lower panel: c = 1 mg/ml; first (left) and second (right) heating cycle. The first heating cycle reduces the fraction of intermolecular β-sheet (1615 $cm^{-1}$).

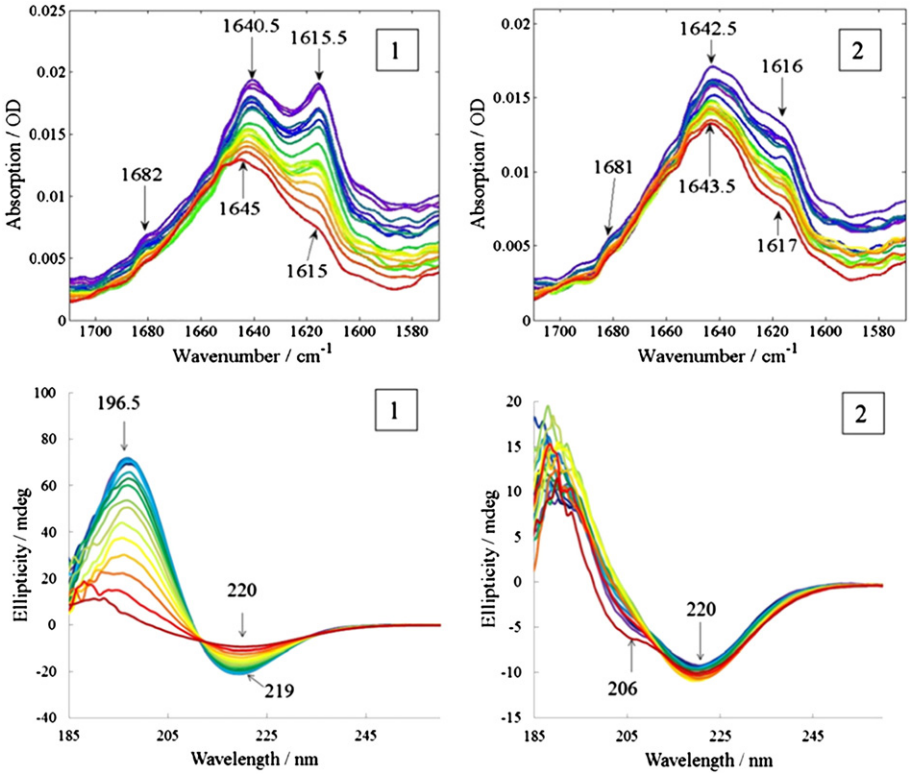


**Fig. 4.** Conformation of $K_2Q_{20}K_2$ measured at c = 0.3 mg/ml from 5 °C (blue) to 90 °C (red). Upper panel: FTIR spectra with first (left) and second (right) heating cycle. Lower panel: CD spectra with first (left) and second (right) heating cycle. Conformation probed by FTIR and CD at the same concentration. Both methods show that the intermolecular β-sheet is much reduced after one heating cycle.

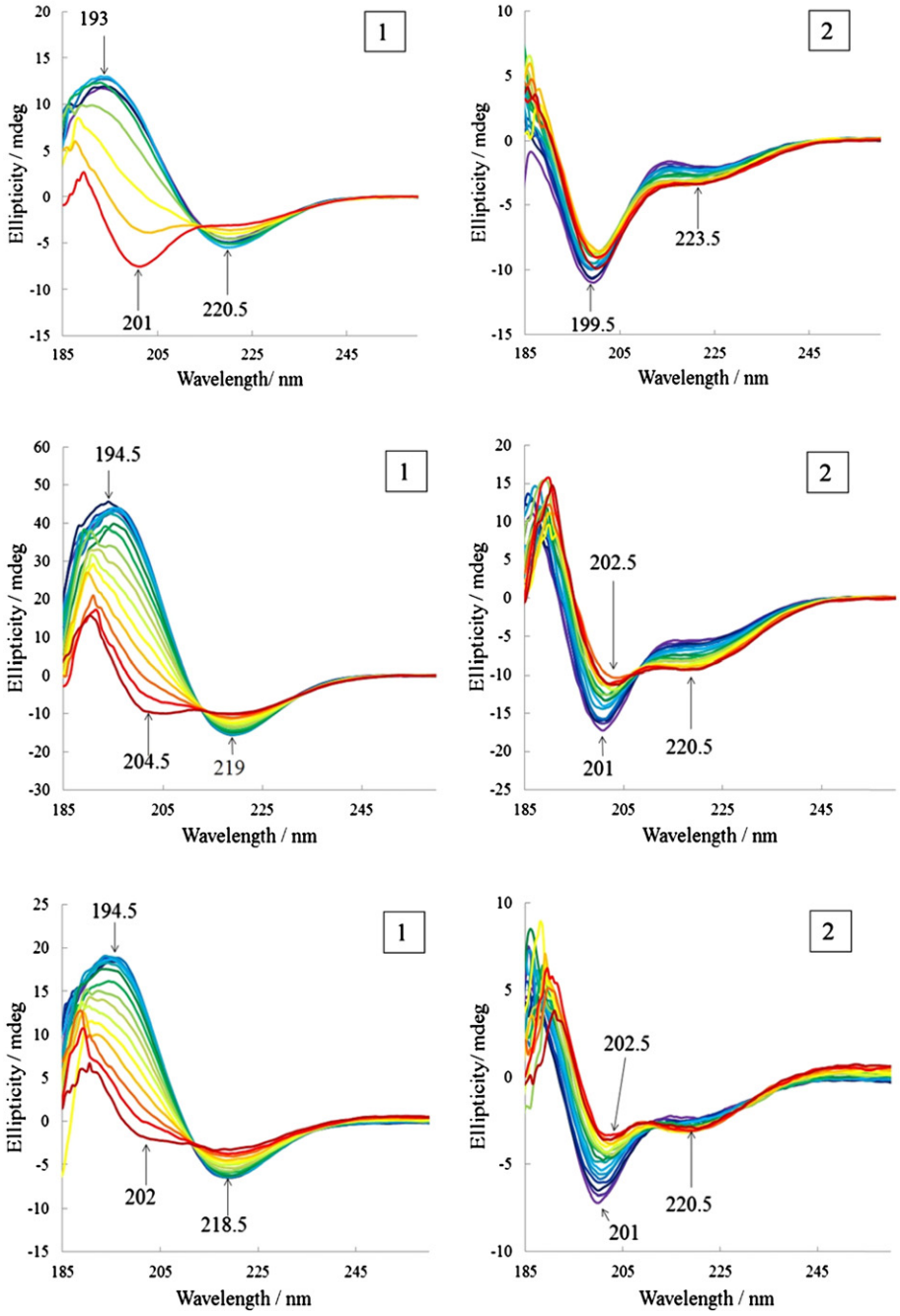


**Fig. 5.** CD spectra of $K_2Q_{20}K_2$ at c = 0.15 mg/ml (upper panel), 0.03 mg/ml (middle panel) and 0.01 mg/ml (lower panel). First (left) and second (right) heating cycles are measured from 5 °C (blue) to 90 °C (red). Reduced concentrations are accessible with CD. At each concentration, the fraction of β-structure is reduced significantly after one heating cycle and random structure is observed in the structural composition. The second heating cycle shows a decrease of random structure upon heating.

maximum at 197.5 nm and a minimum at 219.5 nm. In contrast to $K_2Q_{20}K_2$, no fraction of random structure is observable in the CD-spectra upon heating. Even if the concentration of $K_2Q_{30}K_2$ is lowered to 0.1 mg/ml, no random structure becomes obvious upon heating, but the β-structure is destabilized as can be seen by the temperature-dependent intensity change at 196 nm. However, FTIR-spectra of $K_2Q_{30}K_2$ measured at 0.3 mg/ml do reveal a fraction of random structure that is present in the structural composition.

### 3.2. Impact of the lysines on the conformation

The lysines are introduced to enhance the solubility of the glutamine peptides and potentially influence the conformation of the glutamine sequences. Each peptide consists of the glutamine sequence and 2 lysines at each terminus. For analyzing the impact of lysines, we performed a pD study of $K_2Q_{20}K_2$ (Figs. 8 and 9). The samples were dissolved in $D_2O$ and DCl, $D_3PO_4$ and NaOD were used to adjust the desired pD. Due to the addition of different amount of acids and bases the concentration changed slightly as reflected in absorption intensities. Due to the high solution pK of the lysine side chain (pK ≈ 10.5), a potential impact on conformation is expected to be most dominant at very high pD. Temperature-dependent spectra were measured at 0.3 mg/ml, the concentration feasible for both, FTIR- and CD-spectroscopy.

The CD-spectra measured at pD = 2.5 (Fig. 8) show the same temperature-dependent profile as when the peptide is just dissolved in $D_2O$ resulting in a pD = 2.9 (Fig. 4) as expected. With increasing

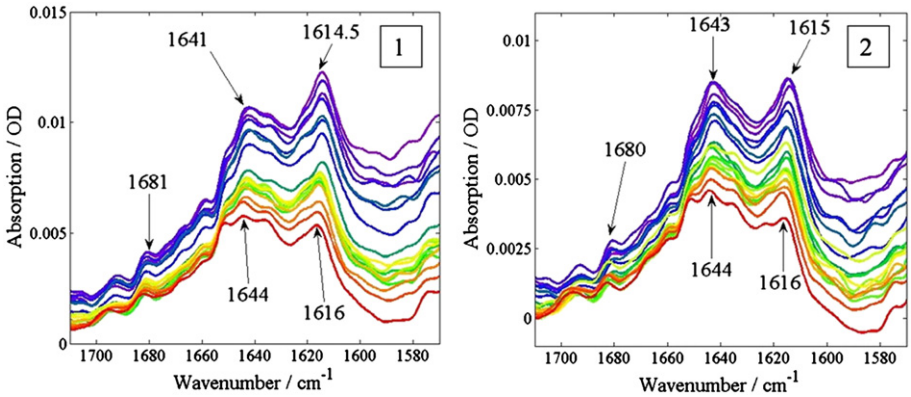


**Fig. 6.** FTIR spectra of $K_2Q_{30}K_2$ with c = 0.3 mg/ml. First (left) and second (right) heating cycle from 5 °C (blue) to 90 °C (red). The fraction of intermolecular β-sheet is significantly increased as compared to $K_2Q_{20}K_2$ (1615 $cm^{-1}$).

pD, the temperature-dependence of the β-sheet band at 197 nm decreases as observable in less intensity change upon heating (Fig. 8). The intermolecular β-sheet becomes more stable and less monomers are released upon heating. At pD = 10.7, the β-sheet band at 199 nm even shows a small intensity increase upon heating. At this high pD value, the lysines are expected to be half neutralized, thus there are less repulsive charges in the sequence and the solubility is decreased.

The same pD study was performed with FTIR spectroscopy (Fig. 9). The water background subtraction became difficult at these low concentrations and water vapor bands could not be avoided. Comparing

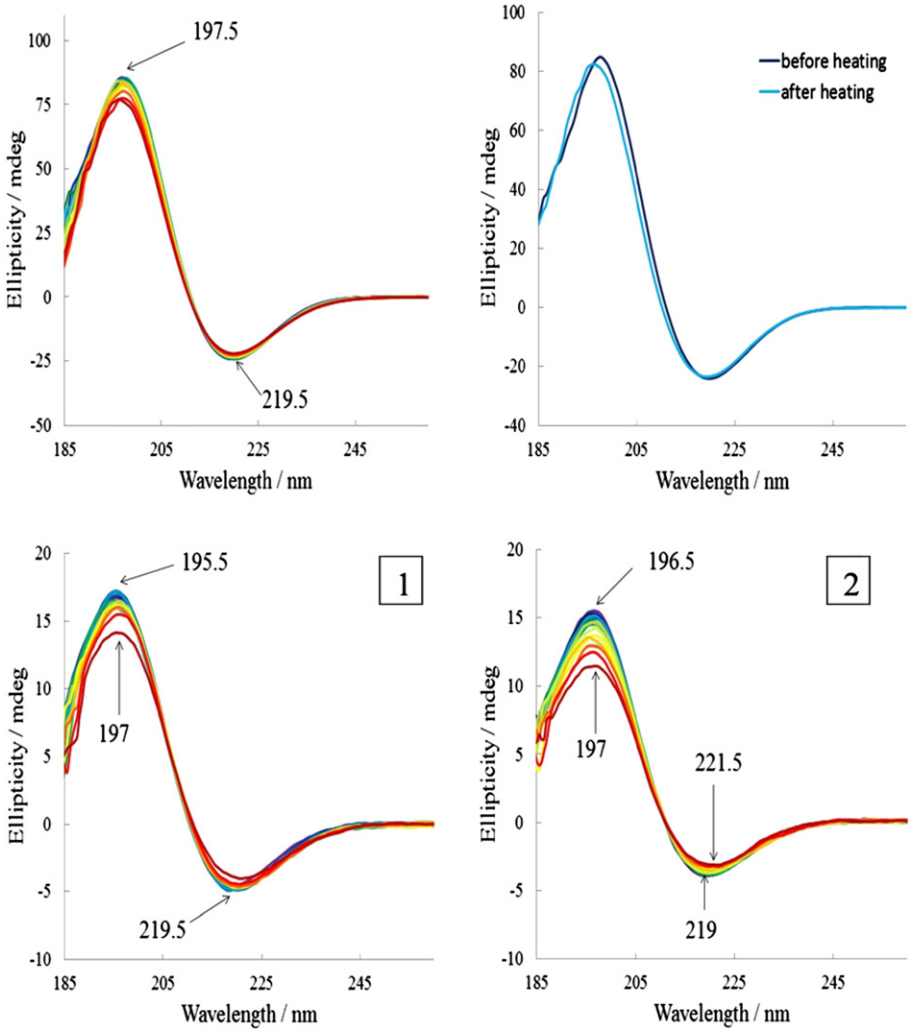


**Fig. 7.** CD spectra of $K_2Q_{30}K_2$. upper panel: c = 0.3 mg/ml measured from 5 °C (blue) to 90 °C (red) (left) and at 20 °C before and after heating (right). Lower panel: c = 0.1 mg/ml measured from 5 °C (blue) to 90 °C (red) with a first (left) and second (right) heating cycle. The CD spectra show solely β-sheet structure that is destabilized upon lowering the concentration.

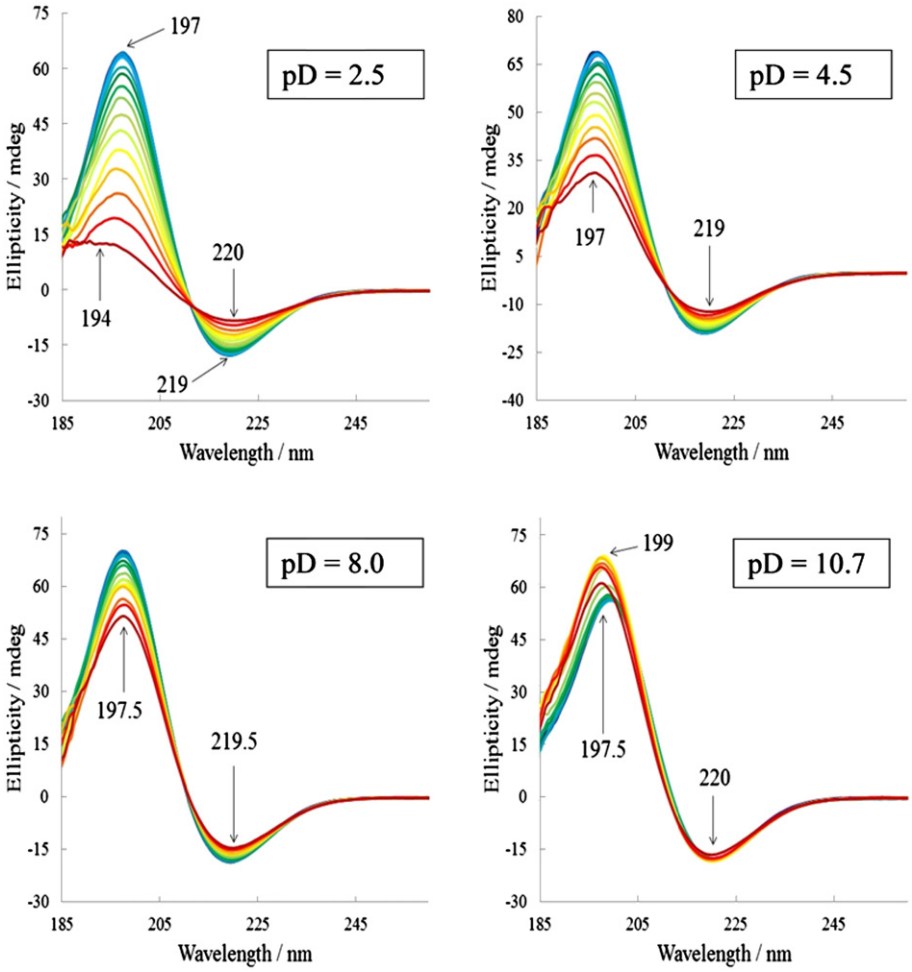


**Fig. 8.** CD spectra of $K_2Q_{20}K_2$ at c = 0.3 mg/ml measured from 5 °C (blue) to 90 °C (red) and with various pD values (pD = 2.5, pD = 4.5, pD = 8.0, pD = 10.7). The thermal stability of the β-sheet is increased with increasing pD.

the ratio of the band at ~1637 $cm^{-1}$ and at ~1613 $cm^{-1}$, it is striking that the intensity of 1613 $cm^{-1}$ increases with increasing pD. As also revealed in the CD-spectra, the β-structures are more stabilized at high pD.

### 3.3. Models

The formation of polyQ fibrils have been observed on a macroscopic scale and different models have been proposed for the aggregation process. In a nucleation elongation model, a thermodynamically unfavorable β-sheet monomer is in equilibrium with bulk disordered monomers. It is suggested to serve as a nucleus in the fibril formation process. An unstructured monomer is bound to the nucleus what results in acquisition of β-structure in the newly added monomer, providing a new elongation site. This fibril formation mechanism is referred as template-assisted elongation [11]. In another model, also called association-conformational conversion model, disordered monomers self-associate via hydrophobic interactions into soluble oligomers. Conformational rearrangement within the oligomer leads to the formation of β-sheets which propagate through the oligomer producing unsoluble fibrillar aggregates [14]. Both models implicate conformational rearrangements that lead to the formation of β-structures and finally to a fibril. It is well agreed that the length of the glutamine sequence is crucial for the disease onset and aggregation in polyQ proteins. The longer the glutamine sequence, the more conformational degrees of freedom and intramolecular contacts are possible. Our spectroscopic results show that the conformation of the polyQ peptides depends on the sequence length. However, the concentration is another critical and important factor.

### 3.4. Sequence length

Both FTIR- and CD-measurements confirm that the shortest studied peptide $K_2Q_{10}K_2$ explores a random structure with no fraction of β-sheet (Fig. 1). This substantiates the assignment of the IR amide I′ band with a band maximum at ~1640 $cm^{-1}$ to random structure, but one should be aware that this band also comprises the carbonyl stretching vibration of the glutamine side chain backbone. The flanking lysines are essential to keep the glutamine sequence soluble. Measurements of $Q_{10}$ peptides without lysines showed a β-sheet structure even at concentrations of 0.01 mg/ml (Supporting Information). In the case of the sequence with 10 glutamines, the lysines obviously prevent the formation of β-sheet. The short monomers will hardly have an intramolecular β-sheet conformation, rather an intermolecular β-sheet will be formed between the monomers. The concentration-dependence of the β-sheet band in the CD spectra of the $Q_{10}$ peptide (without lysines) supports this assumption (Figure S1). By reduction of the concentration and upon heating, the $Q_{10}$ peptide shows a transition to a random structure (Figure S1). The lysines prevent the formation of intermolecular β-sheet. The lysines might also affect the conformation of the monomer, for example by disfavoring the transient formation of loops and turns with nearby C- and N-termini. The impact of the lysines on the monomer conformation is expected to be less, the longer the glutamine sequence is because the fraction of the charged residues in respect to the total glutamine sequence becomes smaller. Additionally, the

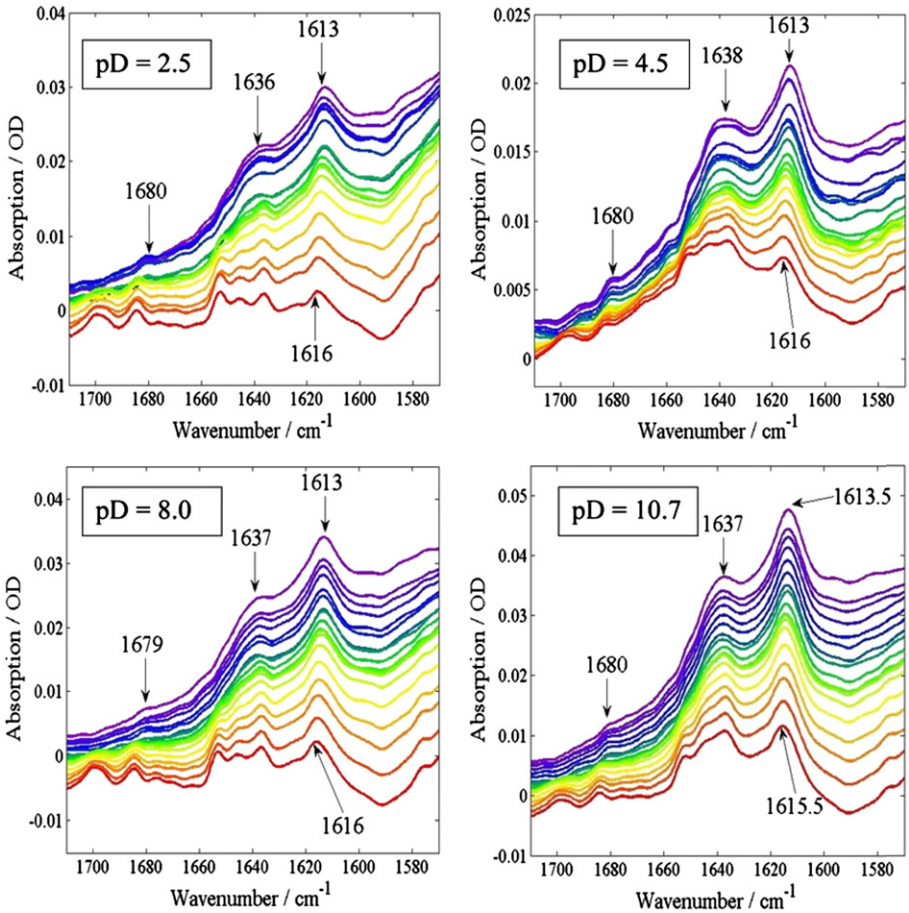


**Fig. 9.** FTIR spectra of $K_2Q_{20}K_2$ at c = 0.3 mg/ml from 5 °C (blue) to 90 °C (red) and with various pD values (pD = 2.5, pD = 4.5, pD = 8.0, pD = 10.7).

repulsive charges are more distant although the effective spatial distance between the terminal charges will not only depend on the number of consecutive glutamines but also on the conformation of the sequence.

The conformational difference of $K_2Q_{20}K_2$ in comparison to the short sequence $K_2Q_{10}K_2$ is obvious due to a significant fraction of β-structure (Fig. 2). We attribute that to intermolecular β-sheets that form between $K_2Q_{20}K_2$ monomers. The fraction of β-sheet is concentration-dependent: the higher the concentration is, the higher is the β-sheet fraction as observable in both, IR- and CD-spectra. Indications for different β-structures is revealed in the IR spectra due to the amide I′ bands at 1691 $cm^{-1}$, 1682 $cm^{-1}$, 1635 $cm^{-1}$ and 1615 $cm^{-1}$ what becomes in particularly obvious at lower concentrations (Figs. 4 and 6). The signal to noise is poor at 0.3 mg/ml (107 μM) which was the lowest accessible concentration that we could measure with IR. Additionally, water vapor bands overlay the IR-spectra that could not completely be subtracted. Thus the assignment of the bands is done very tentatively. In previous studies with well-defined antiparallel β-hairpin peptides containing 12 residues, we observe the amide I′ band component of the intramolecular β-structure at ~1633 $cm^{-1}$ [27,28]. We tentatively assign the band observed at 1635 $cm^{-1}$ to intramolecular β-sheet of the monomers and the band at 1615 $cm^{-1}$ to intermolecular β-sheet formed between the monomers. The steady state spectra do not provide kinetic data about the mechanism, but the presence of different β-structures indicates different steps in fibril formation. It is imaginable that at a sequence length of 20 glutamines, a monomer performs a conformational change to a β-sheet. A β-sheet might have loosened strands towards the termini because of the repulsive lysines. A β-sheet monomer could serve as nucleus for the formation of an extended intermolecular β-sheet between the monomers supporting the template-assisted elongation model [11].

The fibril formation tendency is obviously enhanced in $K_2Q_{30}K_2$. The peptide precipitates to non-soluble aggregates and had to be treated with ultrasound to dissolve it. Several amide I′ band components are resolved in the IR spectra at 0.3 mg/ml concentration (Fig. 6). The assignment of the bands is performed analogously as for $K_2Q_{20}K_2$: the bands at 1692 $cm^{-1}$, 1681 $cm^{-1}$, 1635 $cm^{-1}$ and 1615 $cm^{-1}$ indicate different β-structures, the band at 1641 $cm^{-1}$ carbonyl side chain and random structure. The heating/cooling cycles show that the band at 1615 $cm^{-1}$, assigned to the intermolecular β-sheet, is also reduced after the first heating/cooling. However, the intensity at 1615 $cm^{-1}$ is approximately the same as for the band at 1643 $cm^{-1}$ after re-cooling (Fig. 6, right) indicating that the fraction of β-sheet is much increased in comparison to $K_2Q_{20}K_2$ (Fig. 4, upper panel right). The CD spectra of $K_2Q_{30}K_2$ explore solely a β-structure band (Fig. 7) that decreases marginally in intensity upon heating. In contrast to $K_2Q_{20}K_2$, measured with the same concentration of 0.3 mg/ml (Fig. 4), no transition to a partially random structure is observed, even not when the concentration is further decreased to 0.1 mg/ml (Fig. 7, lower panel). The intermolecular β-sheet structure dominates all $K_2Q_{30}K_2$ CD spectra.

### 3.5. Concentration

$K_2Q_{10}K_2$ explores a random structure at each studied concentration (0.1 mg/ml to 10 mg/ml). The peptide conformation was probed with CD and FTIR and no β-sheet structure was monitored in this

concentration range (Fig. 1). In contrast, β-structure is observed for $K_2Q_{20}K_2$ at each studied concentration (0.01 mg/ml to 10 mg/ml). The fractions of random structure respectively β-structure in the structural composition depends on the concentration. The higher the concentration is, the more the fraction of β-structure increases. By performing several heating/cooling cycles, it has been shown that the fraction of intermolecular β-sheet can be reduced upon heating up once whereas further heating cycles are reversible and do not change the temperature-dependent conformational composition anymore. The band at 1615 $cm^{-1}$ is reduced in intensity after the first heating/cooling cycle revealed in all IR measurements that were performed with concentrations of 10 mg/ml (3.2 mM), 1 mg/ml (320 μM) and 0.3 mg/ml (107 μM) (Figs. 3 and 4). The intensity ratio of the bands at 1639 $cm^{-1}$ (random fraction) and at 1615 $cm^{-1}$ changes significantly if the first heating/cooling cycle is compared with the second one. CD spectra have been measured at reduced concentrations of 0.3 mg/ml (107 μM) (Fig. 4), 0.15 mg/ml (53.5 μM), 0.03 mg/ml (9.6 μM) and 0.01 mg/ml (3.2 μM) (Fig. 5). All CD measurements of $K_2Q_{20}K_2$ show solely β-structure after dissolving. Upon heating, the β-sheet bands at ~195 nm and ~220 nm are reduced. Some less strongly bound monomers seem to be released from the intermolecular β-sheet. The band at ~195 nm decreases to approximately one third. Heating up and re-cooling reveals that the conformation of $K_2Q_{20}K_2$ is composed of both, random structure and β-sheet: a negative band at ~200 nm (random) is observed besides the bands at ~195 nm and ~220 nm (β-sheet) (Figs. 4 and 5, right panels). Unexpectedly, the CD spectra of the second heating/cooling cycles with concentrations of 0.15 mg/ml, 0.03 mg/ml and 0.01 mg/ml show a decrease in random structure (~200 nm) upon heating. In addition, the negative band at ~220 nm gets more intensive. Interestingly, this effect becomes more pronounced at lower concentration. It seems apparently contradictory, that the β-sheet fraction is reduced when the peptide is heated up in the first heating cycle whereas the β-sheet fraction is increased in further heating cycles. It should be noted that in both heating/cooling cycles the ellipticity at ~195 nm is approximately the same at 90 °C. Thus the fraction of β-sheet is approximately the same at 90 °C. A possible explanation would support the nucleation–elongation model [11]: when $K_2Q_{20}K_2$ is dissolved, aggregates of ordered intermolecular β-sheets are formed. The first heating melts the intermolecular β-sheets to a certain degree and monomers are released. At 90 °C, predominantly monomers of random and intramolecular β-sheet structures are present in thermal equilibrium. The lower the concentration is, the more monomers are present and the less intermolecular β-sheet remains. Cooling down increases the fraction of unstructured monomers that are thermodynamically more favorable. The second heating might shift the equilibrium so that some of the unstructured monomers undergo a conformational transition to intramolecular β-sheet structured monomers. A blue-shifted positive band at ~195 nm was interpreted as intermolecular sheet [29], however, different β-structures are difficult to distinguish with CD. In IR, amide I′ components of β-sheets at different frequency positions reflect various β-structures. A low amide I′ frequency in the range of 1615 $cm^{-1}$–1625 $cm^{-1}$ reflects stronger hydrogen bonding and is typically observed in aggregation processes when intermolecular β-sheets are formed. We assigned the dominant band at 1616 $cm^{-1}$ (Fig. 4) to intermolecular β-sheet. The band with a maximum at 1641 $cm^{-1}$ and a shoulder at 1635 $cm^{-1}$ implies the amide I′ components of monomers with random structure and of monomers with intramolecular β-sheet structure. The equilibrium between random monomers and β-sheet structured monomers might be shifted with reduced concentration, like it is observed in the CD measurements, but lower concentrations than 0.3 mg/ml were not accessible for IR measurements. In both, CD and IR measurements, it becomes obvious that the intermolecular β-sheet dominates at high concentrations. Lowering the concentration reveals the structure of the monomers and it seems that the equilibrium between random and β-structured monomers changes with temperature. The concentration–aggregation correlation is even more pronounced for the longer glutamine sequence, $K_2Q_{30}K_2$. At concentrations of 0.3 mg/ml, the CD spectra show exclusively β-sheet structure which is extremely thermostable (Fig. 7). IR spectra at the same concentration (Fig. 6) indicate random and β-structured monomers with a dominant fraction of intermolecular β-sheet (Fig. 4). Decreasing the concentration of $K_2Q_{30}K_2$ from 0.3 mg/ml to 0.1 mg/ml reduces the β-sheet by more than a third as seen in the CD measurements (Fig. 7). The intermolecular β-sheet is definitely dominating the structural composition of $K_2Q_{30}K_2$.

## 4. Conclusion

Our spectroscopic study reveals conformational transitions of glutamine repeats in dependence of the repeat length. Model peptides with 10 consecutive glutamines indicate random-structured monomers whereas β-structures are formed in peptides with 20 respectively 30 glutamines. The observation of different β-structures indicates different steps in fibril formation and that length-dependent conformational transitions of the glutamine sequence precede polyQ fibrillogenesis. Besides the sequence length, our measurements demonstrate that the concentration is another critical factor influencing the conformation of glutamine repeats. The higher the concentration, the higher is the fraction of β-sheet in the structural composition. High local concentrations of polyQ proteins might be a triggering factor in the disease onset besides the pathogenic threshold of the glutamine repeat length.

## Acknowledgements

We gratefully acknowledge the financial support by the Deutsche Forschungsgemeinschaft (SFB 969).

## Appendix A. Supplementary data

Supplementary data to this article can be found online at http://dx.doi.org/10.1016/j.bpc.2013.11.008.

## References

[1] A. Wyttenbach, S.L. Hands, Neurotoxic protein oligomerisation associated with polyglutamine diesease, Acta Neuropathol. 120 (2010) 419–437.
[2] H.A. Popiel, J.R. Burke, W.J. Strittmatter, S. Oishi, N. Fujii, T. Takeuchi, T. Toda, K. Wada, Y. Nagai, The aggregation inhibitor peptide QBP1 as a therapeutic molecule for the polyglutamine neurodegenerative diseases, J. Amino Acids 2011 (2011) 265084.
[3] C.A. Ross, M.A. Poirier, E.E. Wanker, M. Amzel, Polyglutamine fibrillogenesis: the pathway unfolds, Proc. Natl. Acad. Sci. U. S. A. 100 (2003) 1–3.
[4] L. Masino, Polyglutamine and neurodegeneration: structural aspects, Proteins and Peptide Lett. 11 (2004) 239–248.
[5] L.H. Krull, J.S. Wall, Synthetic polypeptides containing side-chain amide groups. water-soluble polymers, Biochemistry 5 (1966) 1521–1527.
[6] M.F. Perutz, T. Johnson, M. Suzuki, J.T. Finch, Glutamine repeats as polar zippers: their possible role in inherited neurodegenerative diseases, Proc. Natl. Acad. Sci. U. S. A. 91 (1994) 5355–5358.
[7] M.F. Perutz, J.T. Finch, J. Berriman, A. Lesk, Amyloid fibers are water-filled nanotubes, Proc. Natl. Acad. Sci. U. S. A. 99 (2002) 5591–5595.
[8] S. Chen, V. Berthelier, W. Yang, R. Wetzel, Polyglutamine aggregation behavior in vitro supports a recruitment mechanism of cytotoxicity, J. Mol. Biol. 311 (2001) 173–182.
[9] S. Chen, R. Wetzel, Solubilization and disaggregation of polyglutamine peptides, Protein Sci. 10 (2001) 887–891.
[10] A.K. Thakur, R. Wetzel, Mutational analysis of the structural organization of polyglutamine aggregates, Proc. Natl. Acad. Sci. U. S. A. 99 (2002) 17014–17019.
[11] S. Chen, F.A. Ferrone, R. Wetzel, Huntington's disease age-of-onset linked to polyglutamine aggregation nucleation, Proc. Natl. Acad. Sci. U. S. A. 99 (2002) 11884–11889.
[12] P. Sikorski, E. Atkins, New model for crystalline polyglutamine assemblies and their connection with amyloid fibrils, Biomacromolecules 6 (2005) 452-432.
[13] M.H. Smith, T.F. Miles, M. Sheehan, K.N. Alfieri, B. Kokona, R. Faitman, Polyglutamine fibrils are formed using a simple designed b-hairpin model, Proteins Struct. Funct. Bioinf. 78 (2010) 1971–1979.
[14] R.H. Walters, R.M. Murphy, Examining polyglutamine peptide length: a connection between collapsed conformation and increased aggregation, J. Mol. Biol. 393 (2009) 978–992.
[15] M. Chopra, A.S. Reddy, N.L. Abbott, J.J.D. Pablo, Folding of polyglutamine chains, J. Chem. Phys. 129 (2008) 135102.

[16] A. Merlino, L. Esposito, L. Vitagliano, Polyglutamine repeats and b-helix structure: molecular dynamics study, Proteins Struct. Funct. Bioinf. 63 (2006) 918–927.
[17] S.D. Khare, F. Ding, K.N. Gwanmesia, N.V. Dokholyan, Molecular origin of polyglutamine aggregation in neurodegenerative diseases, PLoS Comput. Biol. 1 (2005) 230–235.
[18] H. Ogawa, M. Nakano, H. Watanabe, E.B. Starikov, S.M. Rothstein, S. Tanaka, Molecular dynamics simulation study on the structural stabilities of polyglutamine peptides, Comp. Biol. Chem. 32 (2008) 102–110.
[19] S. Barton, R. Jacak, S.D. Khare, F. Ding, N.V. Dokholyan, The length dependence of the PolyQ-mediated protein aggregation, J. Biol. Chem. 282 (2007) 25487–25492.
[20] R. Wetzel, Physical chemistry of polyglutamine: intriguing tales of a monotonous sequence, J. Mol. Biol. 421 (2012) 466–490.
[21] A.K. Covington, M. Paabo, R.A. Robinson, R.G. Bates, Use of the glass electrode in deuterium oxide and the relation between the standardized pD (paD) scale and the operational pH in heavy water, Anal. Chem. 40 (1968) 700–706.
[22] W.Y. Yang, J.W. Pitera, W.S. Swope, M. Gruebele, Heterogenous folding of the trpzip hairpin: full atom simulation and experiment, J. Mol. Biol. 336 (2004) 241–251.
[23] A. Barth, C. Zscherp, What vibrations tell us about proteins, Q. Rev. Biophys. 35 (2002) 369–430.
[24] H. Fabian, D. Naumann, Millisecond-to-minute protein folding/misfolding events monitored by FTIR spectroscopy, in: H. Fabian, D. Naumann (Eds.), Protein Folding and Misfolding, Springer, Berlin Heidelberg, 2012, pp. 53–89.
[25] A. Barth, The infrared absorption of amino acid side chains, Prog. Biophys. Mol. Biol. 74 (2000) 141–173.
[26] M. Jayaraman, R. Kodali, B. Sahoo, A.K. Thakur, A. Mayasundari, R. Mishra, C.B. Peterson, R. Wetzel, Slow amyloid nucleation via a-helix-rich oligomeric intermediates in short polyglutamine-containing huntingtin fragments, J. Mol. Biol. 415 (2012) 881–899.
[27] K. Hauser, C. Krejtschi, R. Huang, L. Wu, T.A. Keiderling, Site-specific relaxation kinetics of a tryptophan zipper hairpin peptide using temperature-jump ir-spectroscopy and isotopic labeling, J. Am. Chem. Soc. 130 (2008) 2984–2992.
[28] K. Hauser, O. Ridderbusch, A. Roy, A. Hellerbach, R. Huang, T.A. Keiderling, Comparison of isotopic substitution methods for equilibrium and T-jump infrared studies of b-hairpin peptide conformation, J. Phys. Chem. B 114 (2010) 11628–11637.
[29] D. Sharma, S. Sharma, S. Pasha, S.K. Brahmachari, Peptide models for inherited neurodegenerative disorders: conformation and aggregation properties of polyglutamine peptides with and without interruptions, FEBS Lett. 456 (1999) 181–185.